Exploring the Role of Altruism in Arrhenotoky with Dynamic Beehive Models

Zachary Nathan, Daniel DiPietro, and Olivia J. Chu

June 29, 2023

Abstract

This study explores the relationship between altruism and arrhenotoky in an evolutionary game theory (EGT) framework, using a dynamic model of beehive populations with three castes: workers, drones, and the queen. Arrhenotoky is a form of asexual reproduction characterized by haplodiploid sex-determination system, found in insects such as the *Hymenoptera*, including bees. In this context, altruism refers to actions taken by an organism that reduce its own fitness to increase the fitness of others. Eusociality, an extreme form of biological altruism resulting in complex social behaviors, is also observed in the *Hymenoptera*. We employ an ordinary differential equation (ODE) model to simulate beehive populations over a range of parameters controlling for altruism in workers and the queen. Our results show that altruistic behaviors are essential for beehive success, with optimal worker altruism ($\epsilon_w = 0.0$) corresponding to the division of labor observed in eusocial species. Furthermore, we find that modest altruism from the queen is also vital for hive survival, emphasizing the delicate balance of these complex social systems. Overall, our findings shed light on the co-evolution of altruism, arrhenotoky, and eusociality in the natural world.

1 Introduction

This work investigates the connection between altruism and arrhenotoky using an evolutionary game theory (EGT) framework. We develop a dynamic model of a beehive environment in which there are three castes – workers, drones, and the queen. Individuals in each of these groups allocate energy within and between them according to variable levels of altruism. Then, the energy surpluses within each caste determine their respective capacities to reproduce. Reproduction occurs in a three-part balance according to the biological system of arrhenotoky.

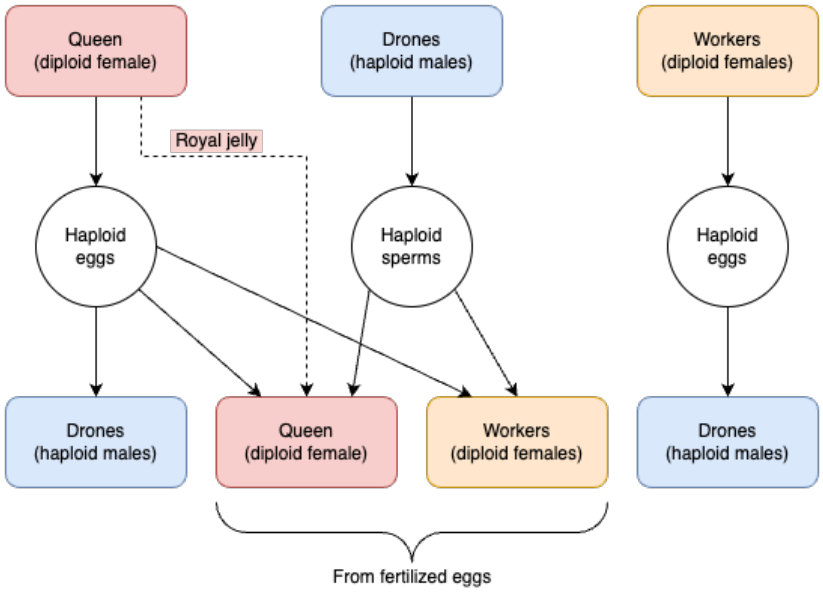

Figure 1: A visual overview of honey bee reproduction via arrhenotoky. Fertilized eggs become diploid females, whereas unfertilized eggs become haploid males. Queens are distinguished from workers by the provision of royal jelly during the larval stage [7].

Although our model can describe any species exhibiting arrhenotoky, we focus our analysis on the honey bee *Apis Mellifera*. Honey bees naturally exhibit arrhenotoky along with complex social structures, making them prime candidates for analyzing the effects of altruism [1]. Honey bees are essential to ecosystems and agriculture worldwide; in the year 2000, *Apis Mellifera* contributed an estimated $14.6 billion via pollination in the United States alone [2]. Furthermore, a wealth of research has been published on the genomics of bees, giving insight into the genetic basis of arrhenotoky and altruism [3, 4, 5]. Finally, we note that bees are difficult to study at the individual level in lab settings, especially compared to flightless species with arrhenotoky such as ants [6].

1.1 Arrhenotoky

Arrhenotoky, or arrhenotokous parthenogenesis, is a form of asexual reproduction distinguished by the haplodiploid sex-determination system. Specifically, unfertilized eggs develop into haploid male offspring, while fertilized eggs develop into diploid female offspring that have twice the number of chromosomes. This phenomenon is characteristic of the *Hymenoptera*, an order of insects including bees, ants, wasps, and sawflies, as well as the *Thysanoptera*, or thrips. Species with arrhenotoky often exhibit distinct genetic and social dynamics, with complex group behaviors including eusociality [1].

With arrhenotoky, the distinctive pathways of reproduction lead to a higher degree of relatedness among female siblings than between parents and offspring. In particular, diploid workers share more genetic material with one another ($\sim$75%) than with their own haploid drone offspring (50%) [8]. Recall that the queen is the mother of all workers as well as most drones; hence, workers inherit half of their genes directly from the queen, and the other half from drones who (almost always) inherit from the queen in turn. Therefore, workers have 75% of their genes in common, or marginally less in the rare case that a drone father was hatched from another worker's egg. This peculiar genetic arrangement gives workers an incentive to act altruistically, as their genes are propagated more effectively via the queen's reproduction than their own [8]. Furthermore, the queen must act altruistically by supporting the drones, who must survive until fertilization to enable the reproduction of workers. Hence, arrhenotoky gives rise to altruism in two distinct forms: workers helping the queen, and the queen helping drones.

1.2 Altruism

In an evolutionary context, altruism is defined as any action taken by an organism that reduces its own fitness in order to increase the fitness of others. Cooperative breeding or hunting, the sharing of food or shelter, and conspicuous predator alarm calls are all examples of altruism in the animal kingdom. Understanding the mechanisms that drive altruistic behavior has significant implications for the study of social organisms and their interactions. Various theories may describe the evolution of altruism, as discussed in section 2.

Perhaps the most extreme form of biological altruism is eusociality, which describes the advanced social organization observed in the *Hymenoptera*, as well as in several other species with and without arrhenotoky [9]. Eusocial behavior is defined by the division of labor into reproductive and non-reproductive castes, cooperative care of offspring, and overlapping generations of adults [10]. Such advanced cooperation allows for colonies to operate much more effectively than the individuals' intelligence would otherwise permit. The *Hymenoptera*, including bees, exhibit both arrhenotoky and eusociality, rendering them compelling objects of study [8].

1.3 Beehive Dynamics

A typical beehive may contain between 10^3 and 10^5 individuals, depending on the species and environment. In all cases, these populations are divided into three distinct castes: the (female) queen, the haploid male drones, the diploid female workers [11].

The queen bee is the leader of the hive, and the mother of most or all of the other bees. With few

exceptions, beehives have a single adult queen who is its largest and longest-living member. She is always surrounded by worker bees, who provide her with food as well as physical protection. The queen's primary purpose is to reproduce; provided enough food and mates, she can lay thousands of eggs per day [8]. These eggs hatch into workers if fertilized, or drones if not.

The main purpose of drone bees is to mate with a queen, enabling the birth of workers via fertilization. As soon as a drone mates with a queen, it dies. Drones are born from unfertilized eggs laid by the queen or workers. Typically, drones constitute anywhere from one to twenty percent of the total beehive population, although this varies seasonally and between species. The secondary role of drones is temperature regulation; their populations peak in the summer, and during the winter, when the hive's resources are most limited, their reproduction ceases entirely [11].

Worker bees are responsible for sustaining the hive, and take on a variety of activities including: collecting nectar and pollen (food), nursing larvae, producing wax and honeycomb, attending to the queen, and defending the hive from invaders. Workers can lay eggs of their own, but these are never fertilized; therefore, workers alone are capable only of producing more drones. This is rare, however, as the vast majority ($> 99.9\%$) of honeybee drones are the queen's direct offspring [8]. Workers themselves are born from eggs which are laid by the queen, then fertilized by drones.

New queen bees are born in a process similar to that of the workers, hatching from fertilized eggs. However, queen larvae are exclusively fed "royal jelly", a protein-rich secretion that enables their development to sexual maturity. In contrast, worker larvae are only fed royal jelly for their first few days, after which they're fed a combination of nectar and pollen known as "bee bread". The queen larvae selection mechanism is not yet fully understood [7]. Once the new queen bee reaches maturity, one of two processes typically occurs. If the old queen no longer releases sufficient pheromones, she is killed by the workers, making way for the new queen in a process called supersedure. Otherwise, the hive undergoes a split; through a process known as swarming, the old queen founds a new hive, taking with her roughly half of the population [11].

2 Related Work

The evolution of altruism and, in particular, the eusocial behaviors exhibited by certain insects, represent a fascinating question in the field of evolutionary biology. A significant body of research supports the theory of inclusive fitness, or kin selection, as the primary driving force behind these behaviors. Hamilton, in his seminal work, proposed the concept of kin selection, suggesting that organisms may increase their own genetic success by aiding relatives, forming the basis of altruistic behavior [12]. Looking at insects, Hughes et al. and Boomsma have presented findings suggesting that monogamy serves as the foundation for the evolution of eusociality, by maximizing relatedness

among descendants [10, 13]. Further studies by Strassman et al., Liao et al., and Queller et al. have reinforced the validity of kin selection as an explanation for eusociality, highlighting the significance of intragenomic conflict [9, 14, 15]. Galbraith et al. provided empirical support for this theory, demonstrating how kin selection predicts intragenomic conflict in honey bees [16].

Alternative theories challenging the primacy of kin selection in explaining the evolution of eusociality have also emerged. For instance, Ratnieks and Helantera argued that coercion better explains the extreme altruism and social inequalities observed in insect societies [8]. A paradigm shift was introduced by Nowak et al., proposing a five-step sequence to explain the evolution of eusociality. Their theory suggested that eusociality arises through (i) group formation, (ii) accumilation of specialized traits, (iii) evolution of eusocial alleles, and (iv) natural selection of emergent traits, leading to (v) between-colony selection shaping life cycles and caste systems [17]. In response to harsh criticism, Nowak and Allen later contended that the phenomena invoked in inclusive fitness theorizing were not relevant to eusociality [18].

This ongoing debate highlights the confounding nature of altruism in evolutionary biology, especially in the case of eusocial insects. Both the inclusive fitness/kin selection theory and the alternative theories contribute valuable insights into understanding the evolution of these phenomena, while encouraging further study. We emphasize that our model does not presuppose any theories, but constitutes an entirely different analytical pathway.

Evolutionary game theory (EGT) provides a useful interdisciplinary framework for the analysis of varied dynamical systems [19]. Our project takes particular inspiration from several EGT studies which have modeled biological systems using game-theoretic simulations [20]. These studies can model the dynamics of cooperation and competition, even among living beings below the level of cognition [21], from altruism in honeybees to facultative cheating in yeast [22]. Other similar studies focus on the dynamics of population growth [23], as well as the stability [24] and shape [25] of population networks.

3 Methods

We develop an ordinary differential equation (ODE) model of arrhenotoky in the beehive environment. This model is implemented in python to simulate beehive populations over a grid of altruism levels.

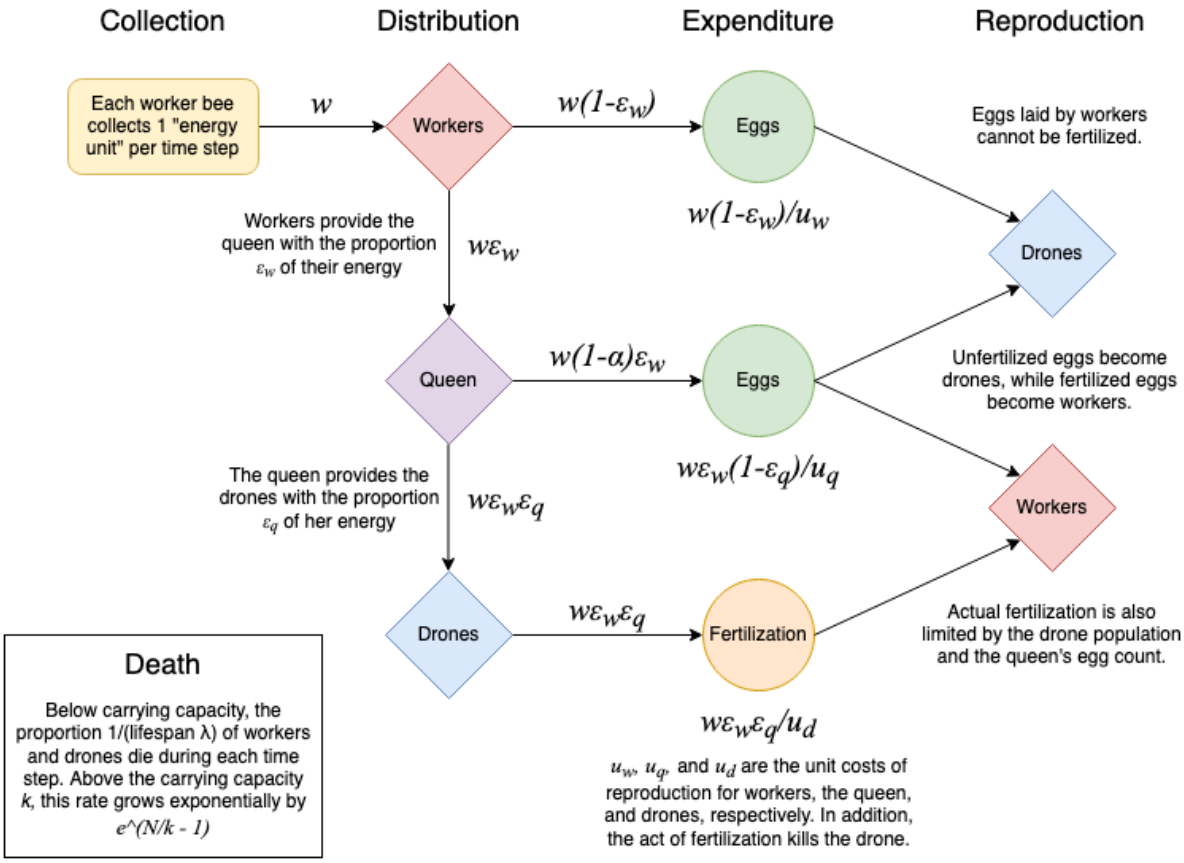

Figure 2: Model overview, illustrating the flow of energy from collection through reproduction. Altruism occurs in the distribution stage. Arrow labels denote energy amounts, while expenditure labels indicate capacity.

3.1 Model

Here we introduce our mathematical model of arrhenotoky reproductive dynamics. This model is formulated within the EGT framework as a public goods game. The workers gather energy, keeping a portion for themselves and altruistically donating the rest to the queen. The queen, in turn, keeps a portion of this energy for herself, donating the rest to the drones. We offer further mathematical details below.

3.1.1 Energy Payoffs

Suppose that each worker bee gathers 1 net unit of energy for the hive at each time step, on average. They keep a proportion $(1-\epsilon_w)$ of this resource for themselves, providing the remaining proportion ϵ_w to the queen. Therefore, the worker population has the following energy pay-off per time step, where w is the number of workers:

$$J_w = w(1-\epsilon_w) \tag{1}$$

Now, the remaining energy $w\epsilon_w$ is provided by the workers to the queen. Much like the workers, she keeps a proportion $(1-\epsilon_q)$ of this energy for herself, releasing the remaining ϵ_q to be shared amongst the drones. So, the queen has the following energy pay-off each round:

$$J_q = w(1-\epsilon_q)\epsilon_w \tag{2}$$

Finally, the collective drone population is left with the following pay-off:

$$J_d = w\epsilon_w\epsilon_q \tag{3}$$

3.1.2 Reproduction

Consider the replication dynamics of this system. As detailed in section 1.3, arrhenotoky dictates that each caste plays a distinct role in the reproductive process:

- Workers produce eggs that develop into drones
- The queen produces eggs that develop into workers if fertilized, or drones if not
- Drones mate with the queen, fertilizing her eggs and dying in the process

In the real world, drones typically mate with queens from different hives, promoting genetic diversity by mingling in drone congregation areas [26]. Our model, however, considers the population dynamics within a single hive, abstracting away the mating locations and genetics. Here, we denote the unit costs of reproduction, in terms of energy, as u_w, u_q, and u_d for the three respective castes. While the actual energy requirements may differ between species, we assert that $u_d < u_q < u_w$. Given that queen bees lay more eggs than workers by several orders of magnitude [8], it follows that their process would be more efficient in terms of the energy expenditure per unit. The low relative cost of drone reproduction arises from Bateman's principle [27]; notwithstanding any flaws in the original experiment, we suppose that "sperm is cheap" in comparison to eggs [28]. Importantly, this unit cost does not take the drone's death into account.

Using these unit costs of reproduction along with the energy payoffs for each caste, we proceed to calculating their respective capacities for reproduction. First, we define E_q as the number of unfertilized eggs produced by the queen:

$$E_q = \frac{J_q}{u_q} \tag{4}$$

Similarly, we define E_w as the number of eggs collectively produced by the workers:

$$E_w = \frac{J_w}{u_w} \tag{5}$$

Finally, we define E_d as the number of eggs collectively fertilized by the drones. This is slightly more complicated, as drones cannot fertilize more eggs than have been produced by the queen, or more eggs than the current number of drones, as each one dies after fertilization. So, where d is the number of drones, we define E_d as:

$$E_d = \min\left(E_q, d, \frac{J_d}{u_d}\right) \tag{6}$$

3.1.3 Death

Whereas queen bees are relatively long-lived, workers and drones die with regularity throughout the lifespan of the hive [8]. Thus, we extend our model to include death dynamics, using the hive's carrying capacity along with expected lifespans for workers and drones. Suppose that workers and drones die after λ_w and λ_d time steps, on average, respectively. In order to achieve these average lifespans, a proportion $\frac{1}{\lambda}$ of each respective caste dies at each time step. That is, $\frac{w}{\lambda_w}$ workers and $\frac{d}{\lambda_d}$ drones die of 'natural causes', provided that the total population N remains below the carrying capacity k.

The carrying capacity k represents the number of bees N that can live safely within a single hive, before excess deaths begin to occur due to resource competition, overcrowding, predation, or other constraints [29]. As long as $N \leq k$, the rate of natural deaths remains unchanged; to enforce the carrying capacity, we increase the rate of natural deaths by the exponential factor $e^{\frac{N}{k}-1}$, determined by the degree to which N exceeds k.

Therefore, we define D_w as the number of worker deaths:

$$D_w = \max\left(1, e^{\frac{N}{k}-1}\right)\frac{w}{\lambda_w} \tag{7}$$

Similarly, we define D_d as the number of drone deaths, recalling that E_d drones die during fertil-

ization:

$$D_d = E_d + \max\left(1, e^{\frac{N}{k}-1}\right)\frac{d}{\lambda_d} \tag{8}$$

3.1.4 Replicator Dynamics

Worker and drone replicator dynamics are written as ordinary differential equations, in the form:

$$\dot{N} = \frac{dN}{dt} = \texttt{births} - \texttt{deaths} \tag{9}$$

We define these replicator equations below, separately for workers and then drones, based on their respective birth and death rates as previously discussed. First, we define $\dot{w}$ for the workers, recalling that they're born from fertilized eggs (E_d):

$$\begin{aligned} \dot{w} &= E_d - D_w \\ \dot{w} &= \min\left(\frac{w(1-\epsilon_q)\epsilon_w}{u_q}, d, \frac{w\epsilon_w\epsilon_q}{u_d}\right) - \max\left(1, e^{\frac{N}{k}-1}\right)\frac{w}{\lambda_w} \end{aligned} \tag{10}$$

Next, we define $\dot{d}$ for the drones, recalling that they're born from unfertilized queen eggs ($E_q - E_d$) as well as worker eggs (E_w):

$$\begin{aligned} \dot{d} &= E_w + (E_q - E_d) - D_d \\ \dot{d} &= \frac{w(1-\epsilon_w)}{u_w} + \frac{w(1-\epsilon_q)\epsilon_w}{u_q} - 2\min\left(\frac{w(1-\epsilon_q)\epsilon_w}{u_q}, d, \frac{w\epsilon_w\epsilon_q}{u_d}\right) - \max\left(1, e^{\frac{N}{k}-1}\right)\frac{d}{\lambda_d} \end{aligned} \tag{11}$$

3.2 Simulation

To observe the effects of altruism, we simulate the beehive model in a grid search over the independent variables ϵ_w and ϵ_q, from 0 (total selfishness) to 1 (total altruism). The model is implemented in python as a system of ODEs, using the `solve_ivp` method from `scipy` to calculate the replicator equations $\dot{w}$ (10) and $\dot{d}$ (11) until time T. Multiprocessing speeds up the grid search, where three results are saved from each instance: the total population, the ratio of drones to workers, and the time of population convergence. To display these results, population heatmaps over the space of ϵ_w and ϵ_q are generated using `seaborn`. We publish our implementation on GitHub, at `https://github.com/ZackNathan/arrhenotoky_simulation`.

The simulation constants are defined in table 1. Generally, these constants do not affect the model's behavior; adjusting their values serves only to shift boundaries and scale results, as shown in section 7. For example, doubling k will simply double the equilibrium populations for all ϵ_w and

Table 1: Simulation constants

Symbol	Value	Description
k	10000	Carrying capacity
T	10000	Simulation time span
w_0	30	Initial worker population
d_0	5	Initial drone population
λ_w	45	Average worker lifespan
λ_d	45	Average drone lifespan
u_w	3.0	Worker reproduction unit cost
u_q	1.5	Queen reproduction unit cost
u_d	0.5	Drone reproduction unit cost

ϵ_q. As such, it makes sense to discuss these populations in terms of k.

4 Results

4.1 Simulation Outcomes

We present the simulation results in fig. 3, illustrating the effects of altruism under arrhenotoky. The heatmaps cover the full range of ϵ_w and ϵ_q from 0 to 1, at increments of 0.0025. We present three significant values from each test: the population totals N_T, compositions $^d/_w$, and times to convergence t_c.

4.1.1 Population Totals

The population total N_T refers to the number of workers w plus the number of drones d at time $t = T$, the end of the simulation. This total does not include the singular queen, whose static population is not affected by the ODEs. In fig. 3b, we present these population totals for all 160,681 simulated pairs of ϵ_w and ϵ_q.

The highest observed population was $34,479$, occurring when $\epsilon_w = 1.0$ and $\epsilon_q = 0.13$. Similar populations exist along a line in the parameter space, in the negative ϵ_w and positive ϵ_q direction. We note the appearance of three high-population "ridges" in the shape of the letter Y, effectively dividing the parameter space into three regions. We explain these regions in section 4.2.1, deriving their boundaries there and in section 4.2.3. Overall, high populations result from plausible levels of altruism across a wide range. Specifically, we observe $N_T > 2k$ for most $\epsilon_w > 0.25$ and $0.1 <$

$\epsilon_q < 0.75$

Interestingly, there are no populations less than the carrying capacity k; simulations with too low ϵ_w or extreme ϵ_q result in populations of zero. We refer to these populations as non-viable, and the edge between them and the viable ones as the *viability boundary*. In our model, reproduction either (i) outpaces death by natural causes until some $N > k$, or (ii) fails before the k threshold, eventually falling to zero. We explain the connection between k and deaths in section 3.1.3, and derive the viability boundary in section 4.2.2.

4.1.2 Population Compositions

Given that beehive populations consist mainly of two distinct castes, workers and drones, we report population compositions d/w in fig. 3c, alongside the totals for each simulation. Here, compositions are measured by the numbers of drones per worker at $t = T$. We plot fig. 3c with a logarithmic scale, in order to better capture the huge variations in d/w across the parameter space. The observed population compositions d/w range from 0.0219 (at $\epsilon_w = 0.98$, $\epsilon_q = 0.9425$) to 26.5 (at $\epsilon_w = 0.8625$, $\epsilon_q = 0.0125$) drones per worker.

A "wedge" shape is apparent in the upper half of the heatmap, with its edges matching the "ridges" observed in fig. 3b. This suggests that d/w is determined by the same underlying factors as N_T. Inside this "wedge" area, population compositions exhibit relatively little variation, with all populations having more workers than drones (that is, $\log d/w < 0$). Moving outside of the "wedge", drones gradually become more prevalent until reaching the viability boundary, beyond which the compositions d/w are undefined. One exception is the upper-right corner (where $\epsilon_w > 0.9$ and $\epsilon_q \approx 0.9$) which has the fewest drones. At such high levels of altruism, the scarce eggs are nearly all fertilized by the over-energetic drones, yielding even fewer drones.

For context, we recall that in real-world beehives, drones typically make up between one and twenty percent of the population, varying by species and by season [11]. This corresponds to compositions d/w between 0.01 and 0.25, or on the scale of fig. 3c, $\log d/w$ between -4.6 and -1.4. The entire "wedge" region falls within this range, as opposed to areas along the edges having low populations N_T.

4.1.3 Times to Convergence

For certain values of ϵ_w and ϵ_q, the simulated populations take vastly longer to converge at a steady state. We present the times to convergence t_c for each simulation in fig. 3d. The concept of convergence is intuitive, but an exact definition is tricky to formulate under the constraints of

`solve_ivp`. Here, we define the time of convergence as the first time t where $|N_t - N_{t-dt}| < 10^{-5}$. The exact time increments dt between consecutive steps are determined by `solve_ivp`, but are guaranteed not to exceed `max_step=2.5`.

As in fig. 3c, we plot fig. 3d with a logarithmic scale to capture the huge variations in t_c. The shortest simulation was $\epsilon_w = 0.9675$ and $\epsilon_q = 0.1625$, converging at $t_c = 65.9$. Conversely, some simulations along the viability boundary fail to converge before ending at $t = T$; these are plotted in white. Simulations near the viability boundary take the longest to converge, with times t_c decreasing on either side. The shortest times to convergence correspond with the same high-population "wedge" area as fig. 3c, reinforcing the connections between these different aspects of the simulation results.

We note that non-viable populations tend to have t_c near the middle of the range. At $\epsilon_w = \epsilon_q = 1.0$, for example, neither the queen nor the workers lay any eggs, with the initial population slowly dying off at a rate of $1/\lambda$ per unit t. In such cases, t_c depends mainly on the definition of "convergence". Here, denoting the convergence threshold of 10^{-5} as δ, we have $t_c = \log_{\frac{\lambda-1}{\lambda}} \frac{\delta\lambda}{N_0}$. Using the lifespan $\lambda = \lambda_w = \lambda_d = 45$ and initial population $N_0 = w_0 + d_0 = 35$, we get a time to convergence of $t_c \approx 500$ for non-reproducing populations. It's interesting that higher-population simulations, under the pressure of excess deaths for $N > k$, tend to converge much faster. Lastly, we observe faint ripples in the "wedge" area of the plot, which we dismiss as artifacts of `solve_ivp` and our definition of convergence.

Taken together, these results serve to illustrate the complex interplay of factors behind arrhenotoky population dynamics. A balancing act is evident, wherein certain combinations of altruism ϵ_w and ϵ_q yield divergent results in terms of the total populations N_t, drone-worker compositions d/w, and times to convergence t_c. We emphasize how the parameter space (or heatmap) is partitioned into distinct regions, including the "wedge" and other viable/non-viable areas. In the next section, we use the ODE model equations from section 3.1 to determine the populations N_t analytically, revealing how these regions are governed by different rules corresponding to the *limiting factors*.

4.2 Mathematical Analysis

Here, the goal is to calculate equilibrium populations given ϵ_w and ϵ_q; that is, the total population of workers and drones upon convergence. This is achieved by solving for $\dot{w} = 0$, separately for each of the three branches in the `min` function of E_d.

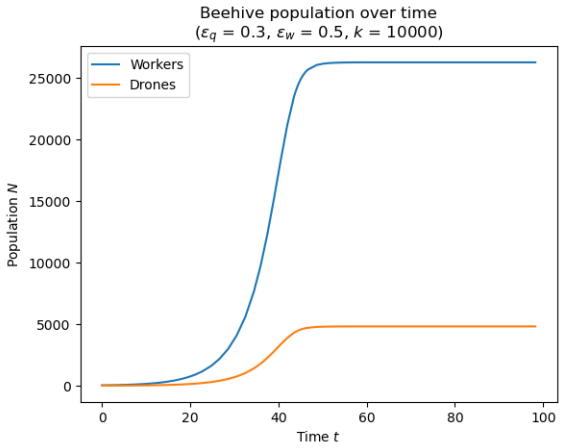

(a) Population growth over time for a single hive with $\epsilon_q = 0.3$ and $\epsilon_w = 0.5$. Truncated at $t = 100$ to highlight the growth curve.

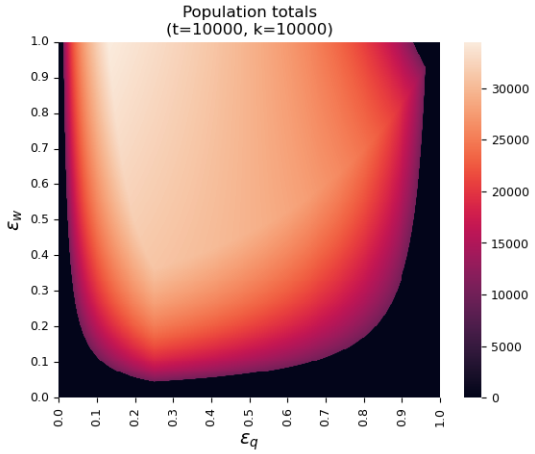

(b) Heatmap showing the final population totals N_T for all values of ϵ_q (queen altruism) and ϵ_w (worker altruism).

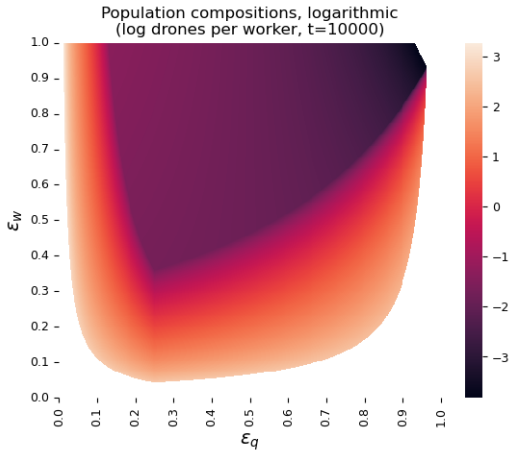

(c) Heatmap showing population compositions (numbers of drones per worker) for non-zero populations. Logarithmic, to improve contrast and highlight the 'wedge' area where workers outnumber drones.

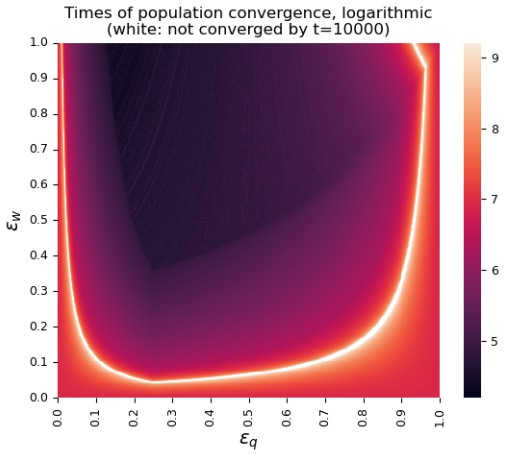

(d) Heatmap showing times t of population convergence at a steady state. Logarithmic to improve contrast. Note how populations along the viability boundary take the longest, or fail to converge by $t = 10000$.

Figure 3: Simulation results.

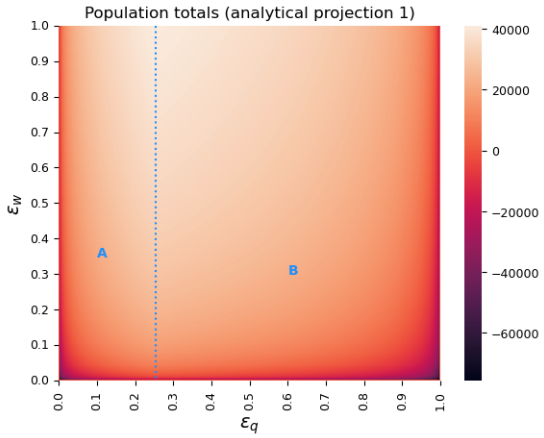

(a) The vertical line at $\epsilon_q = 0.25$ divides the plane between populations limited by drone energy (A) and queen energy (B). We solve for the total population N at equilibrium ($\dot{w} = 0$) in regions A and B, assuming $N \geq k$.

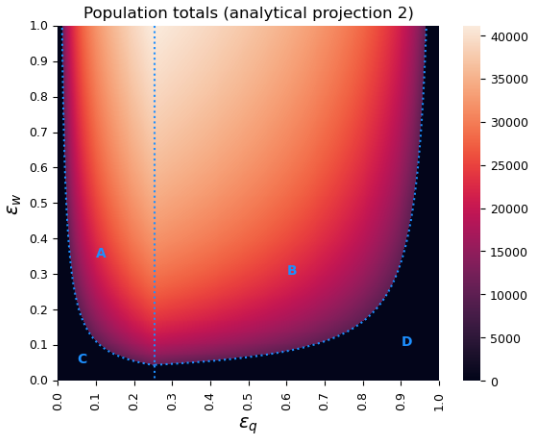

(b) Solving for the viability boundary separates the non-viable regions C and D from the viable regions A and B.

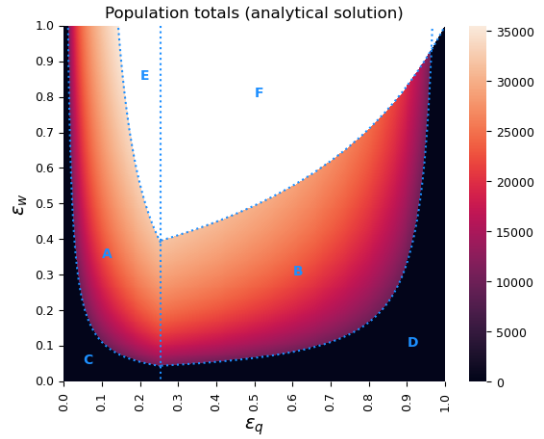

(c) Solving for the limiting factor boundary separates the drone-limited regions E and F from the energy-limited regions A and B. This is the full heatmap of N over the analytically solved regions.

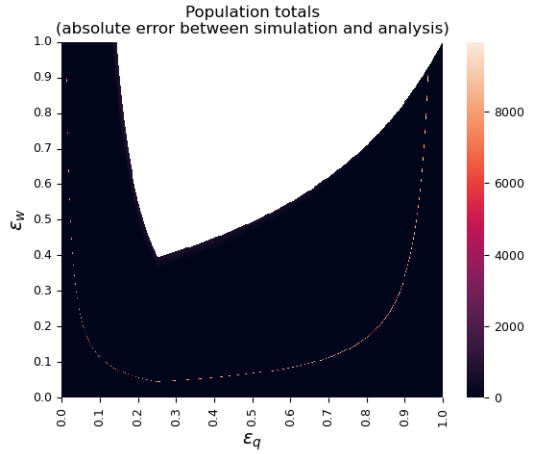

(d) Absolute error between analytical solutions and simulated results over the solved regions. Near-zero everywhere except for the non-converged populations along the viability boundary.

Figure 4: Step-by-step illustration: developing an analytical solution for the total equilibrium population N, in terms of ϵ_q, ϵ_w, and other model parameters.

4.2.1 Limiting Factors

Populations can be limited by three potential factors, corresponding to the three parameters of the `min` function of E_d (6):

Table 2: Limiting factors

Symbol	Description
J_d/u_d	drone fertilization capacity, in terms of energy
E_q	new eggs from the queen, eligible for fertilization
d	drone population, as fertilization results in death

We start by analyzing the case of J_d/u_d, disregarding the difficult case of d for now. Then, this case is defined by the condition:

$$\frac{J_d}{u_d} \leq \frac{J_q}{u_q} \tag{12}$$

$$\epsilon_q \leq 0.25 \tag{13}$$

We find the equilibrium population by solving the worker replicator equation at $\dot{w} = 0$ for the total population $N = w + d$:

$$\dot{w} = E_d - D_w = 0 \tag{14}$$

$$\frac{J_d}{u_d} = \max\left(1, e^{\frac{N}{k}-1}\right)\frac{w}{\lambda_w} \tag{15}$$

For now, we assume that $N \geq k$; that is, $\max\left(1, e^{\frac{N}{k}-1}\right) = e^{\frac{N}{k}-1}$:

$$\frac{w\epsilon_w\epsilon_q}{u_d} = e^{\frac{N}{k}-1}\frac{w}{\lambda_w} \tag{16}$$

$$N = k\left(\ln\left(\frac{\lambda_w}{u_d}\epsilon_w\epsilon_q\right) + 1\right) \tag{17}$$

This equation above applies to region A of the analytical heatmaps in fig. 4, while also proving that equilibrium populations are proportional to k. For the case where $N < k$, see section 4.2.2. Next, we solve for the limiting factor E_q, defined by the inverse of condition (13):

$$\epsilon_q \geq 0.25 \tag{18}$$

Note that at the boundary $\epsilon_q = 0.25$, both cases are equivalent. Proceeding analytically, the results

are similar to (17), with J_q and u_q replacing J_d and u_d:

$$N = k\left(\ln\left(\frac{\lambda_w}{\beta_q}(1-\epsilon_q)\epsilon_w\right)+1\right) \tag{19}$$

This equation above applies to region B of the analytical heatmaps in fig. 4.

4.2.2 Viability

The analysis so far has focused on the cases where the total equilibrium population exceeds the carrying capacity; that is, $N \geq k$, such that death rates are scaled by a factor of $e^{\frac{N}{k}-1}$. However, as some populations fail to reach carrying capacity. In the simulation results, we observe two distinct states of equilibrium:

- Viable: the population reaches k, so the exponential death rate takes effect. Eventually, the increasing death rate catches up to the birth rate, resulting in equilibrium. If not for these excess deaths, unbounded population growth would have occurred.
- Non-viable: the population never reaches k, so the death rate remains at the default of $\frac{1}{\lambda}$. At some point (often $t = 0$), the population hits its peak; here, the birth rate is, by definition, not growing nor greater than the death rate. Although we can't rule out the possibility of an equilibrium where $0 < N < k$, these populations have trended asymptotically toward zero in all applicable simulations.

Therefore, the condition for viability is that the projected equilibrium population is greater than k. Based on (17), we formulate this condition in the case of (13) where $\epsilon_q \leq 0.25$:

$$\ln\left(\frac{\lambda_w}{u_d}\epsilon_q\epsilon_w\right) > 1 \tag{20}$$

$$\epsilon_q\epsilon_w > \frac{u_d}{\lambda_w} \tag{21}$$

This equation above defines the boundary between regions A and C on the analytical heatmaps in fig. 4. Similarly, we formulate this condition in the case of (18) where $\epsilon_q \geq 0.25$, based on (19):

$$\ln\left(\frac{\lambda_w}{u_q}(1-\epsilon_q)\epsilon_w\right) > 1 \tag{22}$$

$$(1-\epsilon_q)\epsilon_w > \frac{u_q}{\lambda_w} \tag{23}$$

This equation above defines the boundary between regions B and D on the analytical heatmaps in fig. 4; regions C and D consist of non-viable populations which always converge to zero.

4.2.3 Boundary Conditions

Next, we proceed to the third limiting factor d, as defined by the condition:

$$E_d = \min\left(E_q, d, \frac{J_d}{u_d}\right) = d \tag{24}$$

We do not have a closed-form solution for the equilibrium population N in this case. However, it is still helpful to express the condition (24) in terms of the simulation parameters. First, we reformulate this condition in the case of (13) where $\epsilon_q \leq 0.25$, and therefore $\frac{J_d}{u_d} \leq \frac{J_q}{u_q}$:

$$d \leq \frac{J_d}{u_d} \leq \frac{J_q}{u_q} \tag{25}$$

$$\frac{d}{w} \leq \frac{\epsilon_q \epsilon_w}{u_d} \tag{26}$$

Intuitively, when the factor limiting population growth is the number of drones, it follows that the ratio of drones to workers must be relatively low. Although we can't describe the equilibrium population directly, we solve for the boundaries between this limiting factor (where $E_d = d$) and the other regions. This is achieved by solving the drone replicator equation at the equilibrium $\dot{d} = 0$ for the population ratio $\frac{d}{w}$, assuming $N \leq k$:

$$\dot{d} = \frac{J_w}{u_w} + \frac{J_q}{u_q} - 2\frac{J_d}{u_d} - \frac{d}{\lambda_d} = 0 \tag{27}$$

Note that $u_w = 2u_q = 6u_d$ under current conditions, as described in table 1:

$$\frac{d}{w} = \frac{\lambda_d}{u_w}\left(1 + \epsilon_w(1 - 14\epsilon_q)\right) \tag{28}$$

Finally, we combine (26) and (28) to define the boundary:

$$6\epsilon_q \epsilon_w = \lambda_d\left(1 + \epsilon_w(1 - 14\epsilon_q)\right) \tag{29}$$

This equation above defines the boundary between regions A and E of the analytical heatmaps in fig. 4. Next, we solve the condition (26) for the remaining boundary in the case of (18), where $\epsilon_q \geq 0.25$ and therefore $\frac{J_q}{u_q} \leq \frac{J_d}{u_d}$:

$$d \leq \frac{J_q}{u_q} \leq \frac{J_d}{u_d} \tag{30}$$

$$\frac{d}{w} \leq \frac{(1-\epsilon_q)\epsilon_w}{u_w} \tag{31}$$

Following the same steps as above, we define the boundary between regions B and F of the analytical heatmaps in fig. 4:

$$\epsilon_w(1-\epsilon_q) = \lambda_d\left(1+\epsilon_w(2\epsilon_q-3)\right) \tag{32}$$

The equilibrium population is thus defined for all solved cases:

$$N = \begin{cases} \begin{cases} \begin{cases} k\left(\ln\left(\frac{\lambda_w}{u_d}\epsilon_q\epsilon_w\right)+1\right) & \text{if } \epsilon_q\epsilon_w > \frac{u_d}{\lambda_w} \\ 0 & \text{otherwise} \end{cases} & \text{if } 6\epsilon_q\epsilon_w < \lambda_d(1+\epsilon_w(1-14\epsilon_q)) \\ \text{unsolved} & \text{otherwise} \end{cases} & \text{if } \epsilon_q \leq 0.25 \\ \begin{cases} k\left(\ln\left(\frac{\lambda_w}{u_q}(1-\epsilon_q)\epsilon_w\right)+1\right) & \text{if } (1-\epsilon_q)\epsilon_w > \frac{u_q}{\lambda_w} \\ 0 & \text{otherwise} \end{cases} & \text{if } \epsilon_w(1-\epsilon_q) < \lambda_d(1+\epsilon_w(2\epsilon_q-3)) \\ \text{unsolved} & \text{otherwise} \end{cases} & \text{otherwise} \end{cases} \tag{33}$$

5 Discussion

Our results serve to illustrate the impact of altruism on arrhenotokous populations. A delicate balancing act is evident, where populations may be limited by various factors depending on the patterns of altruism at play.

Altruism, at some level, is necessary for survival in all populations. Given that workers collect energy on behalf on the entire hive, altruism enables their reproduction via the queen (recall that only the queen's eggs can be fertilized, becoming workers). Otherwise, workers lay eggs that only hatch as drones, preventing the hive from gathering more energy as workers die off without replacement. Hence, all populations where $\epsilon_w = 0$ are non-viable.

Queens must also act with some degree of altruism in order for the populations to survive. If the queen hoards all energy provided by her workers, drones are left without enough energy to fertilize her eggs, jeopardizing the worker population in a manner similar to the above. Conversely, if the queen acts with total selflessness, she lacks the energy required to lay any eggs of her own. Therefore she performs a balancing act, such that populations where $\epsilon_q = 0$ or $\epsilon_q = 1$ are both non-viable.

Trade-offs are introduced into the model by the nature of drone reproduction. Recall that two pathways exist for the birth of drones; unfertilized eggs laid by the queen, and eggs laid by workers

(which cannot be fertilized). This dynamic gives the workers room to act less altruistically, with minimal effect on the total population, as long as the queen acts altruistically enough to let the drones fertilize. This explains the high-population 'ridge' on the heatmap, curving from $\epsilon_q = 0.15$ to $\epsilon_q = 0.25$.

If, however, the workers and queen both act with excessive altruism, energy is wasted as the drones are allocated more than they can use. Given that fertilization results in death, there are simply not enough drones in existence to spend their fertilization 'budget'. This excess energy could have been used by either the workers or the queen to lay more eggs and increase the drone population; therefore, such populations cannot be optimal. It is precisely this region of the heatmap that was not described analytically, given that $\dot{w}$ (10) depends on $\dot{d}$ (11) in these cases.

5.1 Future Directions

We consider several extensions to this project, involving new additions to the model or the relaxation of assumptions. For instance, beehive populations are profoundly affected by seasonal fluctuations, through the changing abundance of food as well as the role of drones in temperature regulation. The dynamic nature of queen bees is another unaddressed question; while one queen suffices for short simulations, the queen-replacing processes of supersedure and swarming are essential to longer-term beehive development [11]. Our model also assumes fixed rates of altruism within each hive, but the introduction of behavior-altering mutations may bring about collective action problems and other interesting dynamics. Lastly, given that our model can already describe other arrhenotokous species, we consider further generalizations to eusocial species up to and including humans, in pursuit of a comprehensive understanding of altruistic behavior in various contexts.

6 Conclusion

We developed an EGT model of arrhenotoky, simulating beehive population dynamics under various levels of altruism. Our results show that levels of altruistic behaviors are among the primary determinants of beehive success. The optimal value of ϵ_w being 0.0 demonstrates the extraordinary evolutionary advantages conferred by eusociality; a hallmark of eusociality is the distinction between reproductive and non-reproductive castes, which is represented in our model by the total lack of eggs laid by workers in simulations where $\epsilon_w = 0.0$. Furthermore, we show that modest altruism from the queen is necessary for the hive's survival, with the most successful populations operating under a delicate balancing act. Taken together, our results serve to illuminate the process by which altruism, arrhenotoky, and eusociality evolved together in the real world.

7 Supplemental Figures

Here, we include additional heatmaps of the simulation results, comparable to those in fig. 3. We vary the model parameters from table 1 to illustrate their effects; in particular, we focus on the unit costs of reproduction u_w, u_q, and u_d. Notably, changing these values moves the boundaries between analytical regions (see fig. 4c), without altering the general pattern.

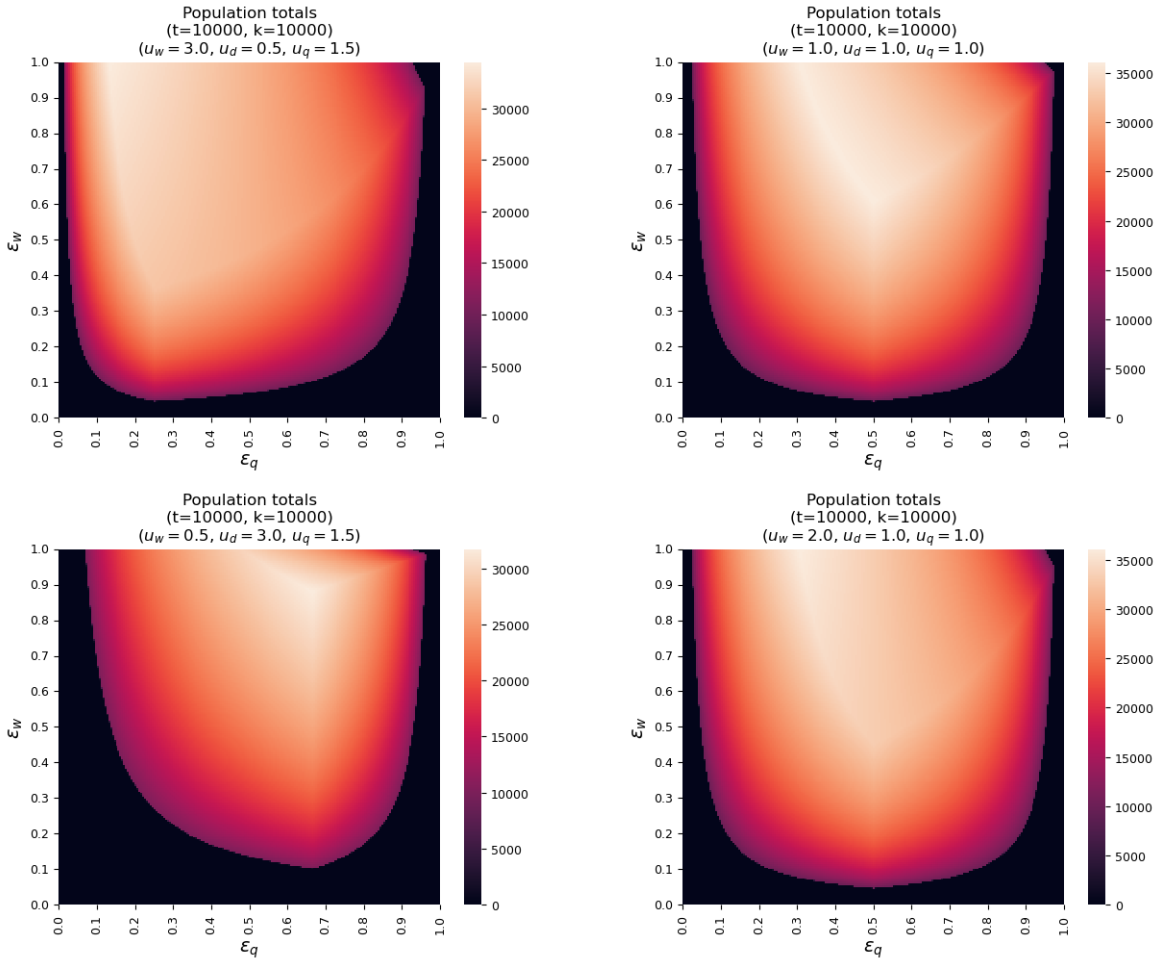

Figure 5: Heatmaps showing the final population totals N_T with varying unit costs of reproduction u_w, u_q, and u_d. The upper left plot shows results with the default parameter values, equivalent to fig. 3b. We denote the parameter values in the titles of each plot.

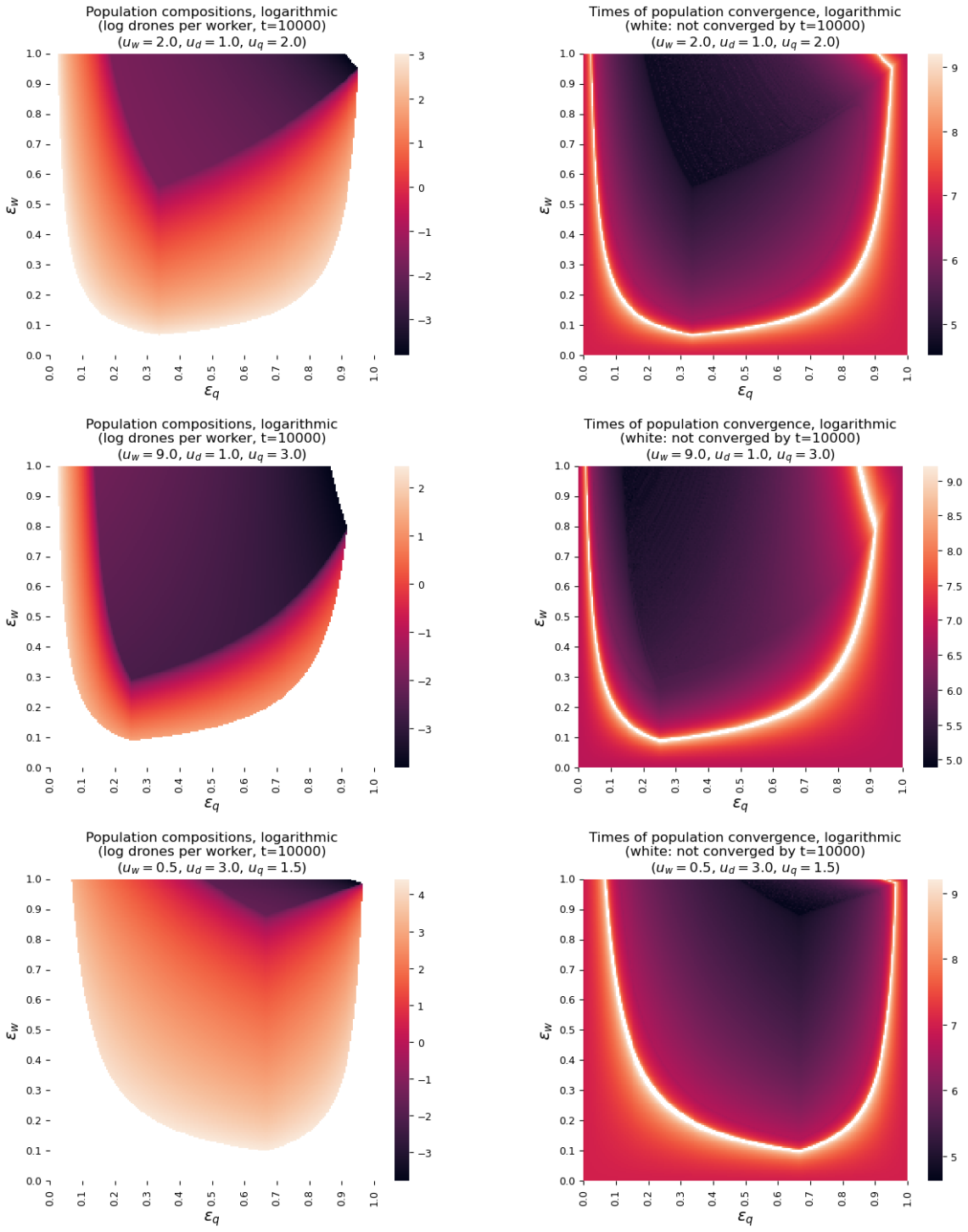

Figure 6: Heatmaps showing the population compositions $^d/_w$ and times of convergence t_c with varying unit costs of reproduction u_w, u_q, and u_d. These results serve to illustrate how divergent parameter values yield heatmaps with diverse shapes and ranges, but always maintaining the same overall pattern of regions seen in fig. 4c. We denote the parameter values in the titles of each plot.

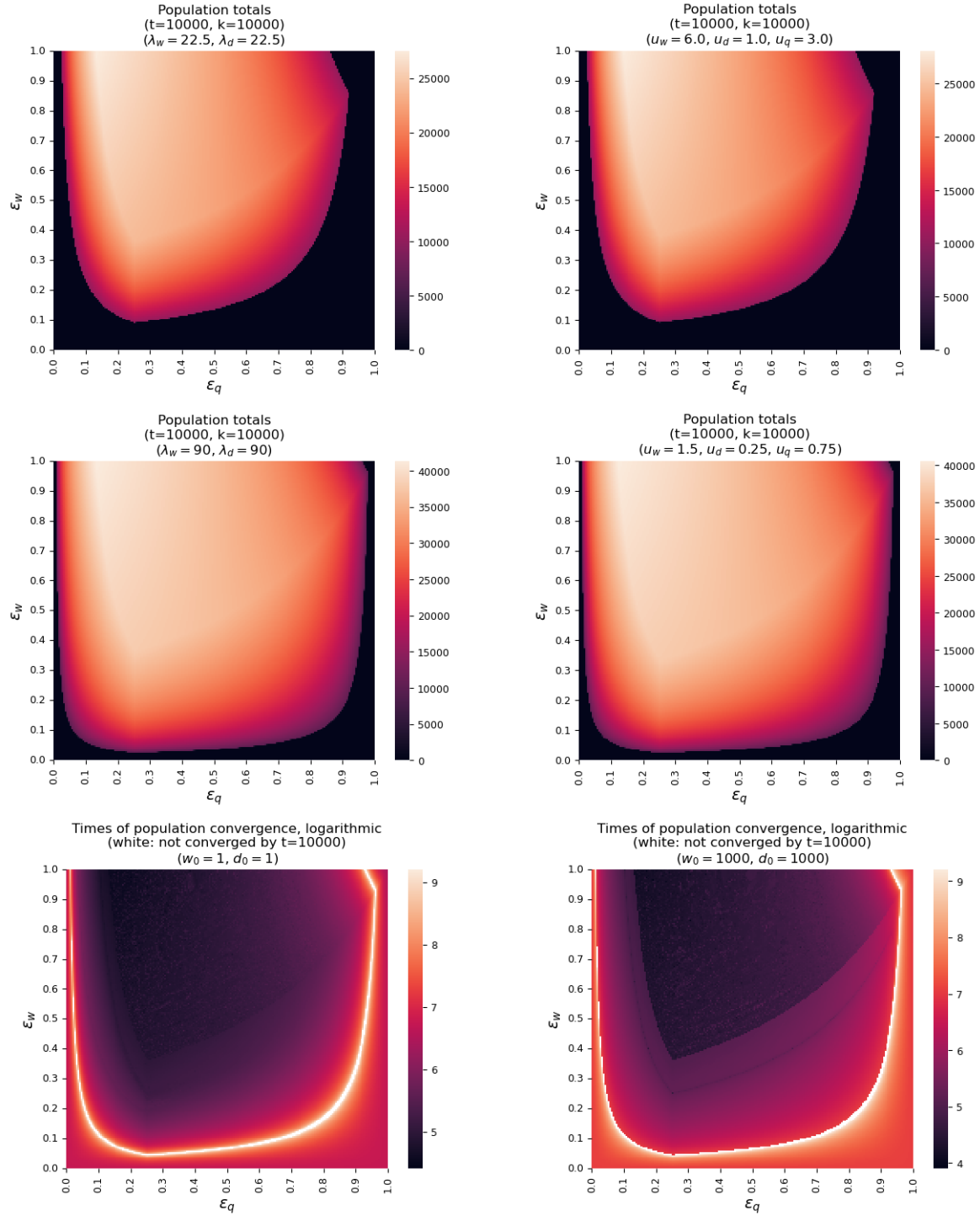

Figure 7: We show that halving the lifespans (λ_w and λ_d) is equivalent to doubling the unit costs; that doubling the lifespans is equivalent to halving the unit costs; and that changing the initial populations (w_0 and d_0) affects only the times of convergence, and only slightly at that.

References

[1] Frances Goudie and Benjamin P. Oldroyd. The distribution of thelytoky, arrhenotoky and androgenesis among castes in the eusocial Hymenoptera. *Insectes Sociaux*, 65(1):5–16, February 2018.

[2] Roger A Morse and Nicholas W Calderone. The value of honey bees as pollinators of us crops in 2000. *Bee culture*, 128(3):1–15, 2000.

[3] Alison McAfee, Jeffery S. Pettis, David R. Tarpy, and Leonard J. Foster. Feminizer and doublesex knock-outs cause honey bees to switch sexes. *PLOS Biology*, 17(5):e3000256, May 2019.

[4] Sean P. Leonard, J. Elijah Powell, Jiri Perutka, Peng Geng, Luke C. Heckmann, Richard D. Horak, Bryan W. Davies, Andrew D. Ellington, Jeffrey E. Barrick, and Nancy A. Moran. Engineered symbionts activate honey bee immunity and limit pathogens. *Science*, 367(6477):573–576, Jan 2020.

[5] Christina M. Grozinger and Amro Zayed. Improving bee health through genomics. *Nature Reviews Genetics*, 21(5):277–291, May 2020.

[6] Toshifumi Kimura, Mizue Ohashi, Karl Crailsheim, Thomas Schmickl, Ryuichi Okada, Gerald Radspieler, and Hidetoshi Ikeno. Development of a New Method to Track Multiple Honey Bees with Complex Behaviors on a Flat Laboratory Arena. *PLOS ONE*, 9(1):e84656, January 2014.

[7] Kegan Zhu, Minghui Liu, Zheng Fu, Zhen Zhou, Yan Kong, Hongwei Liang, Zheguang Lin, Jun Luo, Huoqing Zheng, Ping Wan, Junfeng Zhang, Ke Zen, Jiong Chen, Fuliang Hu, Chen-Yu Zhang, Jie Ren, and Xi Chen. Plant microRNAs in larval food regulate honeybee caste development. *PLOS Genetics*, 13(8):e1006946, August 2017.

[8] Francis L. W. Ratnieks and Heikki Helanterä. The evolution of extreme altruism and inequality in insect societies. *Philosophical Transactions of the Royal Society B: Biological Sciences*, 364(1533):3169–3179, November 2009.

[9] Joan E. Strassmann, Robert E. Page, Gene E. Robinson, and Thomas D. Seeley. Kin selection and eusociality. *Nature*, 471(7339):E5–E6, March 2011.

[10] William O. H. Hughes, Benjamin P. Oldroyd, Madeleine Beekman, and Francis L. W. Ratnieks. Ancestral Monogamy Shows Kin Selection Is Key to the Evolution of Eusociality. *Science*, 320(5880):1213–1216, May 2008.

[11] C.M. Rowland and A.R. McLellan. Seasonal changes of drone numbers in a colony of the honeybee, Apis mellifera. *Ecological Modelling*, 37(3-4):155–166, July 1987.

[12] W. D. Hamilton. The Evolution of Altruistic Behavior. *The American Naturalist*, 97(896):354–356, September 1963.

[13] Jacobus J. Boomsma. Lifetime monogamy and the evolution of eusociality. *Philosophical Transactions of the Royal Society B: Biological Sciences*, 364(1533):3191–3207, November 2009.

[14] Xiaoyun Liao, Stephen Rong, and David C. Queller. Relatedness, Conflict, and the Evolution of Eusociality. *PLOS Biology*, 13(3):e1002098, March 2015.

[15] David C. Queller, Stephen Rong, and Xiaoyun Liao. Some Agreement on Kin Selection and Eusociality? *PLOS Biology*, 13(4):e1002133, April 2015.

[16] David A. Galbraith, Sarah D. Kocher, Tom Glenn, Istvan Albert, Greg J. Hunt, Joan E. Strassmann, David C. Queller, and Christina M. Grozinger. Testing the kinship theory of intragenomic conflict in honey bees (*Apis mellifera*). *Proceedings of the National Academy of Sciences*, 113(4):1020–1025, January 2016.

[17] Martin A. Nowak, Corina E. Tarnita, and Edward O. Wilson. The evolution of eusociality. *Nature*, 466(7310):1057–1062, August 2010.

[18] Martin A. Nowak and Benjamin Allen. Inclusive Fitness Theorizing Invokes Phenomena That Are Not Relevant for the Evolution of Eusociality. *PLOS Biology*, 13(4):e1002134, April 2015.

[19] Arne Traulsen and Nikoleta E. Glynatsi. The future of theoretical evolutionary game theory. *Philosophical Transactions of the Royal Society B: Biological Sciences*, 378(1876):20210508, May 2023.

[20] Peter Hammerstein and Olof Leimar. Evolutionary Game Theory in Biology. In *Handbook of Game Theory with Economic Applications*, volume 4, pages 575–617. Elsevier, 2015.

[21] Sabine Hummert, Katrin Bohl, David Basanta, Andreas Deutsch, Sarah Werner, Günter Theißen, Anja Schroeter, and Stefan Schuster. Evolutionary game theory: cells as players. *Molecular BioSystems*, 10(12):3044–3065, 2014.

[22] Jeff Gore, Hyun Youk, and Alexander Van Oudenaarden. Snowdrift game dynamics and facultative cheating in yeast. *Nature*, 459(7244):253–256, May 2009.

[23] Anna Melbinger, Jonas Cremer, and Erwin Frey. Evolutionary Game Theory in Growing Populations. *Physical Review Letters*, 105(17):178101, October 2010.

[24] Matteo Cavaliere, Sean Sedwards, Corina E. Tarnita, Martin A. Nowak, and Attila Csikász-Nagy. Prosperity is associated with instability in dynamical networks. *Journal of Theoretical Biology*, 299:126–138, April 2012.

[25] Hisashi Ohtsuki, Christoph Hauert, Erez Lieberman, and Martin A. Nowak. A simple rule for the evolution of cooperation on graphs and social networks. *Nature*, 441(7092):502–505, May 2006.

[26] Maria Marta Ayup, Philipp Gärtner, José L. Agosto-Rivera, Peter Marendy, Paulo De Souza, and Alberto Galindo-Cardona. Analysis of honeybee drone activity during the mating season in northwestern argentina. *Insects*, 12(6):566, Jun 2021.

[27] A J Bateman. Intra-sexual selection in Drosophila. *Heredity*, 2(3):349–368, December 1948.

[28] Mats Olsson, Thomas Madsen, and Richard Shine. Is sperm really so cheap? Costs of reproduction in male adders, *Vipera berus*. *Proceedings of the Royal Society of London. Series B: Biological Sciences*, 264(1380):455–459, March 1997.

[29] Ahmed Al-Ghamdi, Nuru Adgaba, Awraris Getachew, and Yilma Tadesse. New approach for determination of an optimum honeybee colony's carrying capacity based on productivity and nectar secretion potential of bee forage species. *Saudi Journal of Biological Sciences*, 23(1):92–100, January 2016.